



HAL
open science

Hidden surface states at non-polar GaN (101⁻0) facets: intrinsic pinning of nanowires

L. Lymparakis, P.H. Weidlich, H. Eisele, M. Schnedler, J.P. Nys, B. Grandidier, D. Stiévenard, R.E. Dunin-Borkowski, J. Neugebauer, P. Ebert

► To cite this version:

L. Lymparakis, P.H. Weidlich, H. Eisele, M. Schnedler, J.P. Nys, et al.. Hidden surface states at non-polar GaN (101⁻0) facets: intrinsic pinning of nanowires. *Applied Physics Letters*, 2013, 103, 152101, 4 p. 10.1063/1.4823723 . hal-00877636

HAL Id: hal-00877636

<https://hal.science/hal-00877636>

Submitted on 27 May 2022

HAL is a multi-disciplinary open access archive for the deposit and dissemination of scientific research documents, whether they are published or not. The documents may come from teaching and research institutions in France or abroad, or from public or private research centers.

L'archive ouverte pluridisciplinaire **HAL**, est destinée au dépôt et à la diffusion de documents scientifiques de niveau recherche, publiés ou non, émanant des établissements d'enseignement et de recherche français ou étrangers, des laboratoires publics ou privés.

Hidden surface states at non-polar GaN (10 $\bar{1}0$) facets: Intrinsic pinning of nanowires

Cite as: Appl. Phys. Lett. **103**, 152101 (2013); <https://doi.org/10.1063/1.4823723>

Submitted: 31 May 2013 • Accepted: 19 July 2013 • Published Online: 07 October 2013

L. Lymparakis, P. H. Weidlich, H. Eisele, et al.



View Online



Export Citation



CrossMark

ARTICLES YOU MAY BE INTERESTED IN

[Microscopic origins of surface states on nitride surfaces](#)

Journal of Applied Physics **101**, 081704 (2007); <https://doi.org/10.1063/1.2722731>

[Luminescence properties of defects in GaN](#)

Journal of Applied Physics **97**, 061301 (2005); <https://doi.org/10.1063/1.1868059>

[Surface states and origin of the Fermi level pinning on nonpolar GaN\(1 \$\bar{1}00\$ \) surfaces](#)

Applied Physics Letters **93**, 192110 (2008); <https://doi.org/10.1063/1.3026743>

Lock-in Amplifiers
up to 600 MHz



Zurich
Instruments



Hidden surface states at non-polar GaN (10 $\bar{1}0$) facets: Intrinsic pinning of nanowires

L. Lymparakis,¹ P. H. Weidlich,² H. Eisele,³ M. Schnedler,² J.-P. Nys,⁴ B. Grandidier,⁴ D. Stiévenard,⁴ R. E. Dunin-Borkowski,² J. Neugebauer,¹ and Ph. Ebert^{2,a)}

¹Computational Materials Department, Max-Planck-Institut für Eisenforschung GmbH, Max-Planck-Str. 1, 40237 Düsseldorf, Germany

²Peter Grünberg Institut, Forschungszentrum Jülich GmbH, 52425 Jülich, Germany

³Institut für Festkörperphysik, Technische Universität Berlin, Hardenbergstr. 36, 10623 Berlin, Germany

⁴Institut d'Electronique, de Microélectronique et de Nanotechnologie, IEMN (CNRS, UMR 8520), Département ISEN, 41 bd Vauban, 59046 Lille Cedex, France

(Received 31 May 2013; accepted 19 July 2013; published online 7 October 2013)

We investigate the electronic structure of the GaN(10 $\bar{1}0$) prototype surface for GaN nanowire sidewalls. We find a paradoxical situation that a surface state at all k points in the bandgap cannot be probed by conventional scanning tunneling microscopy, due to a dispersion characterized by a steep minimum with low density of states (DOS) and an extremely flat maximum with high DOS. Based on an analysis of the decay behavior into the vacuum, we identify experimentally the surface state minimum 0.6 ± 0.2 eV below the bulk conduction band in the gap. Hence, GaN nanowires with clean (10 $\bar{1}0$) sidewall facets are intrinsically pinned. © 2013 AIP Publishing LLC. [<http://dx.doi.org/10.1063/1.4823723>]

Semiconductor nanowires (NWs) have evolved into prime candidates for novel electronic and optoelectronic devices.^{1–4} For example, group III-nitride NWs have excellent optoelectronic properties from the ultraviolet to the red spectral range and hence the potential of becoming highly efficient light emitters^{4–6} as well as chemical sensors.^{7,8} However, the NW geometry leads to an extremely high surface-to-volume ratio compared to conventional semiconductor device structures. Consequently surface-induced effects play a large role for the properties of NWs and the functionality of devices based on them: Surface states critically affect the doping and potential distribution in NWs and the existence of gap states at the NW sidewall facets may lead to non-radiative recombination paths that reduce the quantum efficiency. The most relevant surfaces of wurtzite structure group III-nitride NWs are the non polar m - and a -plane sidewalls facets.^{9,10} Furthermore, growth on these non-polar surfaces is particularly attractive, as detrimental polarization fields that lead to a separation of hole and electron wave function in the active device regions of planar group III-nitride heterostructures can be avoided,¹¹ hence increasing the internal quantum efficiency.¹² As the chemical reactivity during growth (i.e., growth kinetics, incorporation of impurities/dopants and defects) depends sensitively on the electronic¹³ and geometric properties¹⁴ of the surfaces, a detailed knowledge of the energetic position of surface states is critical.

Although GaN is considered as model system for group III-nitride semiconductors, the electronic structure of even the simplest non-polar surface, GaN(10 $\bar{1}0$), and in particular the presence of a surface state within the fundamental bandgap is highly debated, and hence, its electronic behavior remains unclear.¹⁵ Density functional theory (DFT) calculations within the local density approximation (LDA) predict two surface states shifted out of the fundamental

bandgap,^{16,17} whereas recent DFT calculations based on modified pseudopotentials find the upper (empty) surface state in the whole Brillouin zone (BZ) within the bandgap.^{13,18} On the other hand, scanning tunneling microscopy (STM) experiments suggest the absence of surface states in the bandgap,^{17,19} fueling the debate even further. Resolving this issue is, however, critical, as the presence or absence of an intrinsic surface state in the fundamental bandgap strongly affects the surface Fermi level and hence the electrostatics, free carrier concentration, and conductivity of GaN-based NWs.

In this Letter, we combine first principles calculations and scanning tunneling spectroscopy (STS) to clarify the controversial issue of the electronic structure of m -plane GaN surfaces and show that the apparently exotic electronic structure is likely universal for all non-polar surfaces of group III-nitrides and possible of more materials. We find the paradoxical situation that the physically relevant minimum of the intrinsic surface state fully within the bandgap has a very small density of states as compared to bulk states, such that conventional STM mapping modes fail to probe it. This thus far experimentally missed part induces an intrinsic pinning of the Fermi energy and hence modifies the intended doping and potential distribution in nanostructures with non-polar facets.

For our experiments, we cleaved free-standing n -doped GaN samples with dopant concentrations of $(1 - 5) \times 10^{18} \text{ cm}^{-3}$ in ultra high vacuum ($p \approx 1 \times 10^{-8} \text{ Pa}$) to expose a clean and stoichiometric (10 $\bar{1}0$) surface. After cleavage, the samples were directly cooled and investigated at 77 K by STM using tungsten tips. The GaN (10 $\bar{1}0$) cleavage surfaces consisted of large μm -sized terraces, separated typically by one monolayer (ML) high steps. On the 1×1 reconstructed terraces [see inset in Fig. 1(a)] tunneling [$I(V)$] and conductivity (dI/dV) spectra were acquired at constant tip-sample separation z (feedback loop interrupted). The

^{a)}Electronic mail: p.ebert@fz-juelich.de

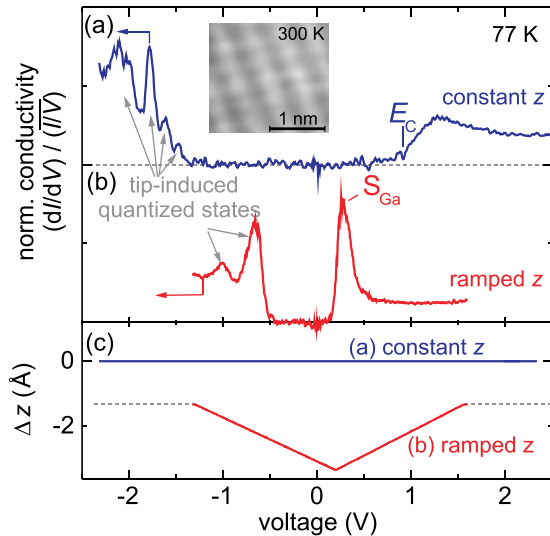


FIG. 1. (a) Normalized differential conductivity spectrum measured at 77 K on the n -type GaN($10\bar{1}0$) surface with constant tip-sample separation z fixed by a set voltage of $V_{\text{set}} = +2.8$ V and set current of $I_{\text{set}} = 150$ pA as shown as blue line labelled constant z in (c) (i.e., $\Delta z = 0$). (b) Same as in (a) but with a reduced tip-sample separation fixed by a set voltage of $V_{\text{set}} = +1.6$ V and set current of $I_{\text{set}} = 200$ pA and an additional ramp approach as shown by the red line in (c) and labelled ramped z . (c) Change of the tip-sample separation Δz as a function of the voltage during the acquisition of the tunneling spectra shown in (a) and (b). Inset: high resolution constant-current STM image measured at 300 K with $V_{\text{set}} = +3$ V and $I_{\text{set}} = 200$ pA.

dI/dV spectra were obtained by extracting the amplitude (and phase) from the Lock-In signal. The normalized conductivity $(dI/dV)/(IV)$ is shown in Fig. 1(a). At negative voltages, a number of peaks occur at voltages well within the bandgap of n -type GaN. These peaks arise from quantized states confined within the tip-induced band bending zone below the tip position.^{20,21} The peaks at negative voltages thus do not reflect the valence band states²² and are of no interest here. Of interest are the empty states. The onset of the empty conduction band states can be observed at +0.9 V, in good agreement with the previous STS data on GaN ($10\bar{1}0$) surfaces.^{17,19} The onset was related to the bulk conduction band minimum (E_C).^{17,19}

The tunneling spectrum in Fig. 1(a) suggests that no intrinsic surface states are present in the fundamental bandgap, as no current is detectable below the onset of the tunnel current into the conduction band. This would at first view favor the calculations which predicted no surface states in the fundamental bandgap.^{16,17}

In order to investigate the electronic structure of the m -plane GaN surface, we have performed first principles calculations within DFT using the LDA and the projector augmented wave approach (PAW).²³ The Ga semicore d states are treated explicitly as valence electrons and an on-site Coulomb interaction U for the aforementioned states has been included.²⁴ This approach improves to a large extent the calculated bandgap by conventional functionals (2.2 eV for LDA and 1.67 eV for generalized gradient approximation (GGA)) and yields a fundamental bandgap of 2.87 eV.²⁴

Careful convergence checks show that thin slabs consisting of less than 24 MLs do not contain enough bulklike material and hence fail to correctly describe the onset of the bulk conduction band as well as to provide a dense mesh of bulk states [compare red and blue dots in Fig. 2(a)]. Thus,

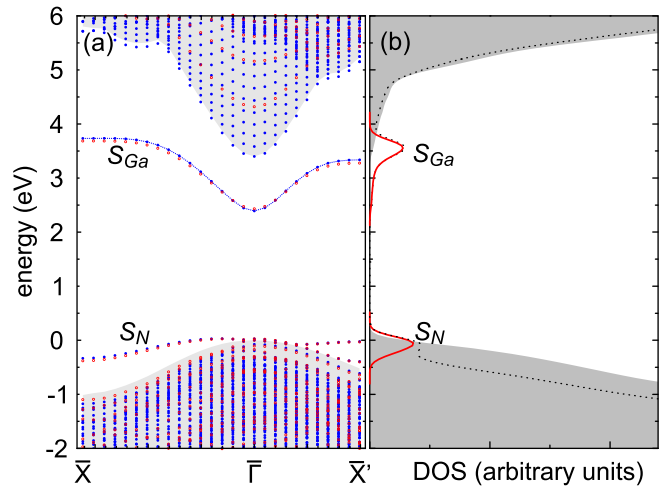


FIG. 2. (a) Band structure of the relaxed GaN ($10\bar{1}0$) surface along high symmetry lines of the surface Brillouin zone calculated with a slab consisting of 48 MLs (blue dots) and 12 MLs (red dots). The solid blue line indicates the unoccupied surface state (S_{Ga}). S_N denotes the N-derived occupied surface state. (b) DOS of the 48 MLs slab (dotted line). The red solid curves indicate the DOS arising from the surface states. In (a) and (b), the grey shaded areas denote the projected bulk band structure and DOS, respectively. In both cases, the top of the bulk valence band is set to 0, and the bulk conduction band has been rigidly shifted to meet the experimental bandgap of GaN.

thin slabs (i) underestimate the density of states (DOS) at this energy region and (ii) fail to describe the decay of the bulk band edge states into the vacuum. Unfortunately, thick slabs are not only computationally more expensive but also suffer from the charge sloshing²⁵ along the slab preventing to reach electronic charge self-consistency. In order to tackle this, we modify and extend the approach originally developed by Engels *et al.* to accelerate self-consistent calculations of thick slabs.²⁶ We first calculated the charge density of a slab consisting of 24 MLs (i.e., ≈ 2.5 nm) self-consistently. Then, the slab is opened in the middle, and additional 24 bulklike GaN MLs have been inserted, yielding a slab with a thickness of 48 MLs (i.e., ≈ 5 nm). Second, non-self-consistent calculations keeping the charge density fixed and using 187 k -points in the irreducible part of the surface BZ were performed. Comparison with the projected bulk band structure [gray area in Fig. 2(a)] shows that this approach describes the bottom of the bulk conduction band with 0.15 eV accuracy. A detailed analysis of the energetic position and dispersion of the surface state as well as on the decay of the states into the vacuum showed that this approach describes the dispersion and the decay with an accuracy better than 0.1 eV and 1%, respectively.

The calculated band structure and the corresponding DOS are shown in Fig. 2. The GaN($10\bar{1}0$) surface exhibits a N-derived occupied state (S_N) at the onset of the bulk valence band (E_V) at 0 eV and a Ga-derived unoccupied s -type state (S_{Ga}) 2.4 eV above E_V . The empty Ga-derived surface state is in the whole BZ in the fundamental bandgap and never resonant with the bulk bands. Surprisingly, this surface state is apparently not probed by STM measurements. In order to understand the failure of conventional STM to probe the surface state, we analyze in detail the surface electronic structure. First, the dispersion in Fig. 2(a) reveals that the energy of the unoccupied surface state exhibits a strong

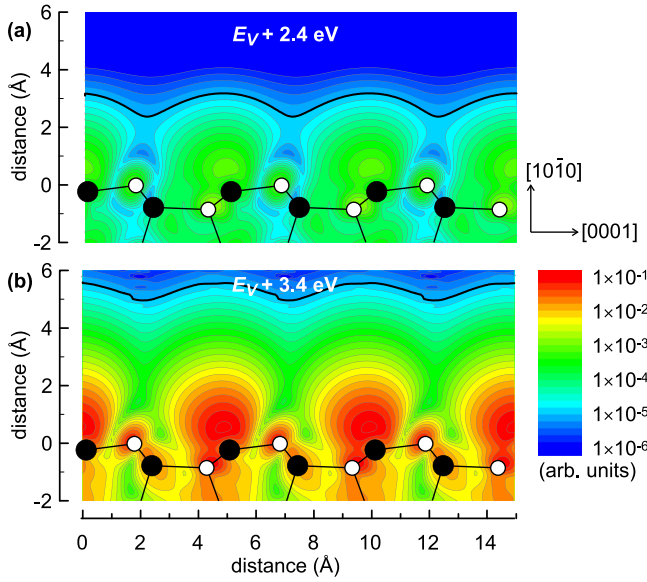


FIG. 3. Integrated partial charge density along the $\langle 11\bar{2}0 \rangle$ direction of the states at energies of (a) $E_V + 2.4\text{ eV}$ (surface state onset) and (b) $E_C (= E_V + 3.4\text{ eV})$ (onset of bulk conduction band). In both cases the partial charge density is the superposition of all states weighted with a Gaussian with standard deviation of 25 meV centered at the corresponding energy value. The z -scale is logarithmic and the same in (a) and (b). Thicker contour lines indicate isolines of the same value in (a) and (b). Open (filled) circles represent the N (Ga) atoms.

dependence on the parallel wave vector: Both strong and almost flat dispersions around the $\bar{\Gamma}$ point and the edges of the BZ, respectively, occur. This affects the DOS shown in Fig. 2(b): The surface state exhibits a long tail with a low DOS into the fundamental bandgap, while the main peak overlaps with the onset of the bulk conduction band.

In a second step, we investigate the decay of the different states into the vacuum, since the STM probes the DOS far above the surface in the vacuum. The extension of the states into the vacuum can be illustrated using the charge density distribution of two groups of states energetically located at the onset of (i) the surface state S_{Ga} (i.e., 2.4 eV above E_V) and (ii) the conduction band E_C (i.e., 3.4 eV above E_V). The corresponding contour plots are shown in Fig. 3. In both cases, a localization at the Ga surface atoms is revealed with the corresponding lobe extended into the vacuum. However, surprisingly the charge density arising from the states at $E_V + 3.4\text{ eV}$ is much stronger and extends farthest into vacuum. Hence, STM will primarily probe states at the bulk conduction band minimum and not the minimum of the surface state. This is a direct consequence of the above mentioned strong dispersion of the surface state around the $\bar{\Gamma}$ point and the corresponding low DOS tail.

The partial charge densities integrated over the $(10\bar{1}0)$ plane in Fig. 4 show that the two groups of states follow a similar decay. But, the states at the bulk conduction band minimum have an intensity more than two orders of magnitude higher than the surface state minimum. To probe equally strong signals for both states in tunneling spectra one has to approach the tip toward the surface by 2.4 \AA (see separation of dashed lines). This is also visible in Fig. 3(a) as a smaller extent of the surface state minimum into the vacuum. Furthermore, the decay of the surface state at different points of the BZ (inset of Fig. 4) shows that the surface state decays

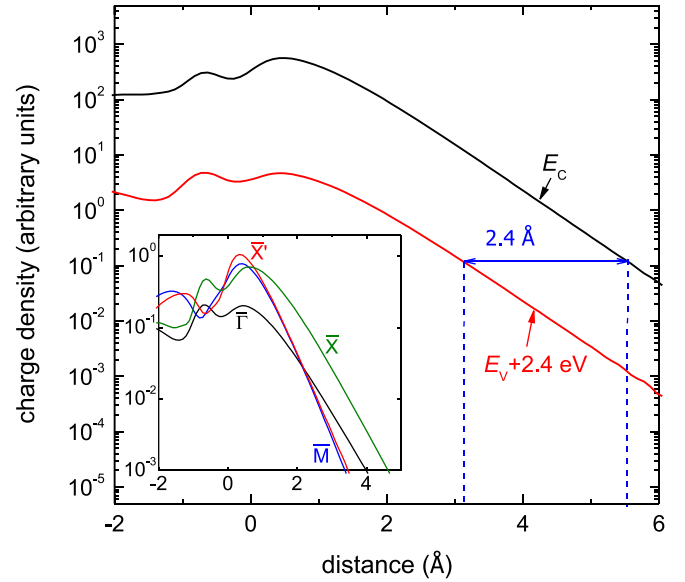


FIG. 4. Decay of the partial charge density integrated over the $(10\bar{1}0)$ planes arising from the states at the onset of S_{Ga} at $E_V + 2.4\text{ eV}$ (red/lower line) and those with energies at the bulk conduction band edge E_C (black/upper line). The same Gaussian weighted superposition approach as in Fig. 3 has been applied. Inset: Decay of the surface state for different high symmetry k -points of the surface Brillouin zone. In both diagrams, the topmost N surface atom is located at the distance 0. Positive and negative values of the distance correspond to vacuum and bulk regions, respectively.

slowest at the $\bar{\Gamma}$ point. At the edge of the BZ the decay is always faster. Hence, at the \bar{X}' and \bar{M} points, the DOS is negligible as compared to that at the $\bar{\Gamma}$ point. However, at the \bar{X} point, the DOS is still higher until an extrapolated distance of $\sim 11\text{ \AA}$ from the surface, due to the extremely flat dispersion of the surface state at the \bar{X} point.

In order to experimentally probe the physically relevant part of the surface state, i.e., its minimum in the bandgap, based on the aforementioned *ab initio* calculations, we increased the sensitivity of our STM experiment by approaching the tip toward the surface. The tip-sample separation is reduced first by increasing the set current and decreasing the set voltage (equivalent to $\Delta z = -1.37\text{ \AA}$). Second, by an additional ramp (shown in Fig. 1(c) as red curve), we reduce the separation further up to 2 \AA , while keeping the tunnel current always within the dynamic range of the preamplifier.²⁷ The normalized conductivity spectrum at this up to 3.37 \AA reduced tip-sample separation is shown in Fig. 1(b). At negative voltages, again peaks arise from quantized states confined in the tip-induced band bending zone facing the tip. Their energy is shifted, since the reduced tip-sample separation increases the band bending, hence increasing the confinement energy of the band bending zone. The interesting feature is the appearance of a strong peak centered at $+0.25\text{ V}$. The peak indicates the presence on a surface state within the fundamental bandgap roughly $0.6 \pm 0.2\text{ eV}$ below E_C (neglecting possible band bending effects).²⁸ This agrees well with the energy position between 0.7 ^{13,18} and 1 eV below E_C calculated for the empty surface state. Thus, we assign this peak to the onset of the surface state at the $\bar{\Gamma}$ point. Note, the experimentally necessary reduction of the tip-sample separation by up to 3.37 \AA agrees with the calculated value of 2.4 \AA for which the DOS at the minima of the surface state and bulk conduction band is

predicted to be identical. The absence of features related to the bulk band edge in Fig. 1(b) has been shown to arise from spreading resistance effects in the transport of carriers at small tip-sample separations.²⁹ The band edge reappears if larger tip-sample voltages are used.

In conclusion, using a detailed *ab initio* analysis combined with tunneling spectroscopy, we were able to clarify the electronic structure of the non-polar *m*-plane GaN surface. The most debated but physically most relevant minimum of the empty surface state is well below the conduction band minimum within the fundamental bandgap, but has an surprisingly low DOS due to a particularly unusual dispersion and decay characteristic: A steep dispersion minimum with low DOS near the $\bar{\Gamma}$ point hidden in conventional STM faces an extremely flat area with high DOS at the edge of the BZ. As a result, the non-polar GaN(10 $\bar{1}$ 0) surface is intrinsically pinned at $(E_C - 0.6) \pm 0.2$ eV.

Nanostructures with non-polar sidewall facets (e.g., almost all nanowires) intrinsically encounter difficulties in defining the potential distribution within the nanostructure by pure doping. Even overgrowth by a wide gap material need to be handled with caution, as a similar electronic structure, i.e., a dispersion of the surface state within the gap with a steep minimum near the $\bar{\Gamma}$ point and extremely flat maximum at the edge of the BZ, is found for both the *a*- and *m*-plane surfaces of GaN and AlN (InN too, but unpinned).^{18,30} Hence, all non-polar surfaces of wurtzite structure GaN and AlN are pinned and will affect the potential within nanowires.

The authors thank the Deutsche Forschungsgemeinschaft under Grant Nos. Eb 197/5-1 and Ei 788/2-1 and the Impuls- und Vernetzungsfonds of the Helmholtz-Gemeinschaft Deutscher Forschungszentren under Grant No. HIRG-0014 for financial support. L.L. acknowledges support from EU FP7-PEOPLE-IAPP-2008 through Grant No. SINOPLE 230765.

¹T. Mårtensson, C. P. T. Svensson, B. A. Wacaser, M. W. Larsson, W. Seifert, K. Deppert, A. Gustafsson, L. R. Wallenberg, and L. R. Samuelson, *Nano Lett.* **4**, 1987 (2004).

²M. G. Lagally and R. H. Blick, *Nature* **432**, 450 (2004).

³S. Li and A. Waag, *J. Appl. Phys.* **111**, 071101 (2012).

⁴J. C. Johnson, H.-J. Choi, K. P. Knutsen, R. D. Schaller, P. Yang, and R. J. Saykally, *Nature Mater.* **1**, 106 (2002).

⁵F. Qian, Y. Li, S. Gradečak, H.-G. Park, Y. Dong, Y. Ding, Z. L. Wang, and C. M. Lieber, *Nature Mater.* **7**, 701 (2008).

⁶H. Sekiguchi, K. Kishino, and A. Kikuchi, *Appl. Phys. Lett.* **96**, 231104 (2010).

⁷V. Dobrokhotov, D. N. McIlroy, M. G. Norton, A. Abuzir, W. J. Yeh, I. Stevenson, R. Pouy, J. Bochenek, M. Cartwright, L. Wang, J. Dawson, M. Beaux, and C. Berven, *J. Appl. Phys.* **99**, 104302 (2006).

⁸G. S. Aluri, A. Motayed, A. V. Davydov, V. P. Oleshko, K. A. Bertness, N. A. Sanford, and M. V. Rao, *Nanotechnology* **22**, 295503 (2011).

⁹K. A. Bertness, A. Roshko, L. M. Mansfield, T. Harvey, and N. A. Sanford, *J. Cryst. Growth* **300**, 94 (2007).

¹⁰L. Largeau, D. L. Dheeraj, M. Tchernycheva, G. E. Cirlin, and J. Harmand, *Nanotechnology* **19**, 155704 (2008).

¹¹P. Waltereit, O. Brandt, A. Trampert, H. Grahn, J. Menniger, M. Ramsteiner, M. Reiche, and K. Ploog, *Nature* **406**, 865 (2000).

¹²A. E. Romanov, T. J. Baker, S. Nakamura, and J. S. Speck, *J. Appl. Phys.* **100**, 023522 (2006).

¹³C. G. Van de Walle and D. Segev, *J. Appl. Phys.* **101**, 081704 (2007).

¹⁴L. Lymperakis and J. Neugebauer, *Phys. Rev. B* **79**, 241308(R) (2009).

¹⁵H. Eisele and Ph. Ebert, *Phys. Status Solidi (RRL)* **6**, 359 (2012).

¹⁶J. E. Northrup and J. Neugebauer, *Phys. Rev. B* **53**, R10477 (1996).

¹⁷M. Bertelli, P. Löptien, M. Wenderoth, A. Rizzi, R. G. Ulbrich, M. C. Righi, A. Ferretti, L. Martin-Samos, C. M. Bertoni, and A. Catellani, *Phys. Rev. B* **80**, 115324 (2009).

¹⁸D. Segev and C. G. Van de Walle, *Europhys. Lett.* **76**, 305 (2006).

¹⁹L. Ivanova, S. Borisova, H. Eisele, M. Dähne, A. Laubsch, and Ph. Ebert, *Appl. Phys. Lett.* **93**, 192110 (2008).

²⁰R. Dombrowski, C. Steinebach, C. Wittneven, M. Morgenstern, and R. Wiesendanger, *Phys. Rev. B* **59**, 8043 (1999).

²¹M. Wenderoth, M. A. Rosentreter, K. J. Engel, A. J. Heinrich, M. A. Schneidez, and R. G. Ulbrich, *Europhys. Lett.* **45**, 579 (1999).

²²Ph. Ebert, L. Ivanova, and H. Eisele, *Phys. Rev. B* **80**, 085316 (2009).

²³G. Kresse and J. Hafner, *Phys. Rev. B* **47**, 558 (1993); G. Kresse and J. Furthmüller, *Phys. Rev. B* **54**, 11169 (1996).

²⁴A. Janotti, D. Segev, and C. G. Van de Walle, *Phys. Rev. B* **74**, 045202 (2006).

²⁵G. P. Kerker, *Phys. Rev. B* **23**, 3082 (1981).

²⁶B. Engels, P. Richard, K. Schroeder, S. Blügel, Ph. Ebert, and K. Urban, *Phys. Rev. B* **58**, 7799 (1998).

²⁷P. Mårtensson and R. M. Feenstra, *Phys. Rev. B* **39**, 7744 (1989).

²⁸Since the concentration of extrinsic surface defects is small on the freshly cleaved GaN(10 $\bar{1}$ 0) surfaces, only intrinsic surface states can be at the origin of the measured surface state within the bandgap.

²⁹V. Ramachandran and R. M. Feenstra, *Phys. Rev. Lett.* **82**, 1000 (1999).

³⁰M. S. Miao, A. Janotti, and C. G. V. de Walle, *Phys. Rev. B* **80**, 155319 (2009).